ISSN 1023-1935, Russian Journal of Electrochemistry, 2024, Vol. 60, No. 8, pp. 670–678. © Pleiades Publishing, Ltd., 2024.

Electrocatalytic Activity of Sr-Doped Lanthanum Cobaltate for Oxygen Evolution Reaction in Alkaline Medium

B. Lal[a], * and P. Chauhan[a]

[a] *Department of Chemistry Institute of Applied Sciences and Humanities, GLA University Mathura, Mathura, 281406 India*

**e-mail: basant.lal@gla.ac.in*

Received August 7, 2023; revised February 7, 2024; accepted February 20, 2024

Abstract—$La_{1-x}Sr_xCoO_3$ ($x = 0.1$, 0.2, 0.3, 0.4, and 0.5) were prepared by the alginic acid sol–gel route and characterized by thermo gravimetric analysis (TGA), Fourier transform infrared (FT-IR), X-ray diffraction (XRD), and scanning electron microscope (SEM) techniques. The electrocatalytic activity of fabricated oxide electrodes (Ni/oxide) was studied for oxygen evolution reaction (OER) in an alkaline medium. The cyclic voltammetry of oxide electrodes shows a pair of redox couple at anodic peak potential (E_{pa}) = 400 ± 6 mV and cathodic peak potential (E_{pc}) = 296 ± 8 mV. The observed values of electrode kinetic parameters such as the Tafel slope (b) lie between 91 and 126 mV dec^{-1} and current density (j) lie between 17.0–73.1 mA cm^{-2} at 0.85 V. The Sr-substitution in lanthanum cobaltate matrix improve electrocatalytic activity for OER in an alkaline medium and maximum improvement was observed in the case of 0.4 mol Sr-substituted oxide. The order of reaction (p) with respect to the concentration of [OH^-] is found unity and the highly negative value of entropy of the reaction indicated the oxygen evolution follows the same mechanism and involves the adsorption of the reaction intermediate.

Keywords: cyclic voltammetry, electrocatalysis, linear sweep voltammetry, perovskite oxide, Tafel polarization, oxygen evolution reaction

DOI: 10.1134/S1023193524700253

INTRODUCTION

$La_{1-x}Sr_xCoO_3$ ($0 \le x \le 0.5$) are considered good candidates for electrocatalytic points of view among perovskite families [1]. If the oxide is prepared using low-temperature techniques, it can be used as a low-cost electrode for water electrolysis in an alkaline environment. The oxides prepared by the conventional high-temperature ceramic method for oxygen evolution have limited electrochemical surface area and decreased homogeneity. To improve the electrocatalytic properties, perovskite oxides were prepared by spray drying [2], co-precipitation [3], freeze-drying [4], microwave-assisted [5], sonochemical reactions [6], sol–gel combustion [7], citrate precursor techniques [8], the hydrothermal method [9] and microemulsion precursors [10]. The oxide film was deposited onto the conductive support by the spray pyrolysis [11] and thermal decomposition [12] and studied their electrocatalytic properties for oxygen evolution reaction. Novel acceptable low-temperature methods utilizing nitrite cyanide and hydroxide solid solutions [13] and organic amorphous methods such as citrate and malic acid as precursors were reported in the literature previously.

These oxides were studied using electrochemical methods, and it was discovered that they were significantly more active for oxygen evolution than other oxides made using more traditional high-temperature processes. Perovskite-type oxides of the $La_{1-x}Sr_xCoO_3$ variety are useful as electrode materials for a variety of technologically significant processes, including the production of O_2, Cl_2, chlorates, O_2 reduction, H_2 evolution, etc. [14], Metal-substituted perovskites-type oxides are used as catalysts in a variety of reactions, including the Haber process for the breakdown of H_2O_2 [15], the preparation of NH_3 [16], energy storage devices [17], gas sensors [18], electrochemical sensors [19], multilayer-chip inductors [20], energy conversion devices [21], clean energy applications [22], etc. These oxide nanoparticles are helpful in a variety of catalytic activities, such as the oxygen evolution reaction, the measurement of hydrogen peroxide, anode electrocatalyst, lithium-ion battery components, and energy storage (supercapacitor) [23–27]. Among these families of perovskite-type oxides, $La_{1-x}Sr_xCoO_3$ are more common and less expensive owing to its component elements, Co, La, and Sr. These oxides have a variety of valences, larger surface area, and are non-toxic to human health. They are best for electrocatalysis because they produce charge ordering, superconductivity, spin-dependent transport, and ferroelectricity [28–30]. This oxide is made using a less expensive, environmentally friendly pro-

cess. In, present investigation an effort have been made to synthesize low cost and ecofriendly perovskite type oxide by using alginic acid sol-gel auto combustion method, $La_{1-x}Sr_xCoO_3$ nanoparticles (x = 0.1, 0.2, 0.3, 0.4, and 0.5 mol) for their electrocatalytic behaviour for oxygen evolution reaction in the KOH solution.

EXPERIMENTAL

Strontium substituted lanthanum cobaltate ($La_{1-x}Sr_xCoO_3$) was prepared by alginic acid (Labogens) sol–gel route using strontium nitrate $Sr(NO_3)_2$ (AR, Sigma Aldrich, 99%) lanthanum nitrate $La(NO_3)_3$ (AR, Sigma Aldrich, 99.999%) and cobalt nitrate $Co(NO_3)_2$ (AR, Sigma Aldrich, 98%). The nitrate salts (0.02 M) were taken in their stoichiometric ratios and dissolved in 200 mL double distilled water with stirring and also prepared the alginic acid solution 4 w/o separately in 200 mL double distilled water and added the liquor ammonia to maintain pH 7 for complete dissolution of alginic acid. The resultants solutions were stirred separately at room temperature till homogeneity for an hour. The resulting homogenous brown solution of alginic acid was added into the metal salt solution in drop wise manner with constant stirring until the milky brown solution, and then evaporated at 100°C to get a black lustrous gel. The desired perovskite-type oxides were obtained by the thermal decomposition of metal–alginic acid composite gel at 600°C for 5 h in an electrical muffle furnace.

To determine the thermal stability of the gel form, the gel of metal salt with alginic acid precursor was subjected to thermal gravimetric analysis (model: Mettler Toledo TGA/DSC 3+) in the temperature range between 25 and 600°C with the constant flow of nitrogen. FT-IR spectroscopy and XRD spectroscopy were used to confirm the formation of a stable perovskite oxide phase. The FT-IR spectrum of perovskite oxide was recorded between wavenumber 400 and 4000 cm^{-1} using the IRSPIRIT-T Shimadzu spectrophotometer and the for XRD powder pattern, D8 Advance BRUKER, CuK_α-the source of radiation, λ = 1.54059 Å and examined from $2\theta = 20°$ to 80°. Morphology and crystallite size were observed by scanning electron microscopy with the help of a Zeiss Gemini SEM 500 thermal field emission. For the electrochemical study, the oxide electrode was fabricated by the repeated coatings of oxide slurry prepared by mixing 2 drops of glycerol and 100 mg of oxide onto the one side pre-treated nickel plate in concentrated HCl, rinsed in acetone and washed with double distilled water and subsequently sintered in an electrical furnace at 300°C for 1 h to get desired oxide loading (~5–6 mg cm^{-2}). For electrical contact, a flattened end of copper wire was connected with the non-coated side of the nickel plate using silver paste and mounted with epoxy resin (Araldite) leaving an exposed oxide area of approximately 0.5 cm^{-2}. Electrocatalytic properties of the fabricated electrode were performed in a single compartment pyrex glass cell provided with Ni/oxide electrode as a working electrode, graphite rod as a counter electrode and Hg/HgO/1 M KOH (0.098V vs. NHE) as a reference electrode using the CHI electrochemical work station.

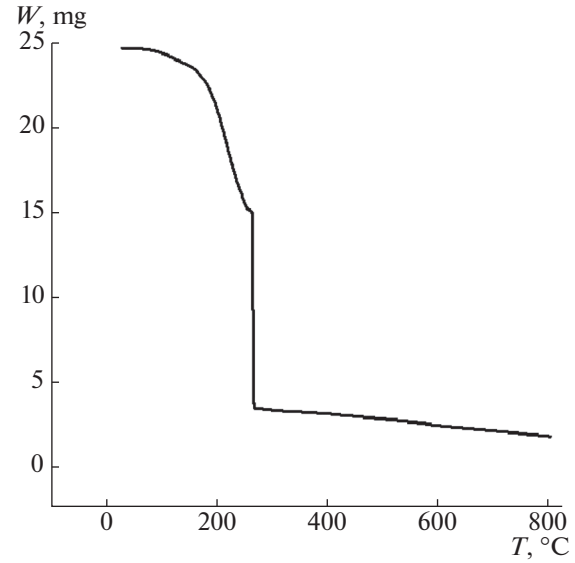

Fig. 1. TGA of the gel obtained at 100°C for $La_{0.6}Sr_{0.4}CoO_3$.

RESULTS AND DISCUSSION

Thermogravimetric Analysis

TGA of metal–alginic acid gel (La–Sr–Co–alginate complex) was recorded in an inert atmosphere in the temperature range of 25 to 600°C and shown in Fig. 1. From the thermogram it is obvious that the weight loss in sample below 200°C due to removal of water from sample and it became stable with very less reduction in weight due decomposition of organic moiety of sample occurred above 270°C that indicated the formation of stable perovskite-type oxide occurs upon heating of the sample.

FT-IR Studies

In order to ensure the formation of the perovskite-type oxide sample was analyzed by the FT-IR technique in wavenumber region between 400–4000 cm^{-1}. The IR spectra of 0.1, 0.4 and 0.5 mol Sr-substituted lanthanum cobaltates are shown in Fig. 2. Sr-substituted lanthanum cobaltate oxides characteristic peaks in all the cases show the absorption bands at 563 cm^{-1} due to the banding mode of vibration of $LaCoO_3$. Another band of the absorption peak at 419 cm^{-1} indicates the formation of O–Co–O and La–O–Co, representing the generation of $LaCoO_3$ crystalline phase

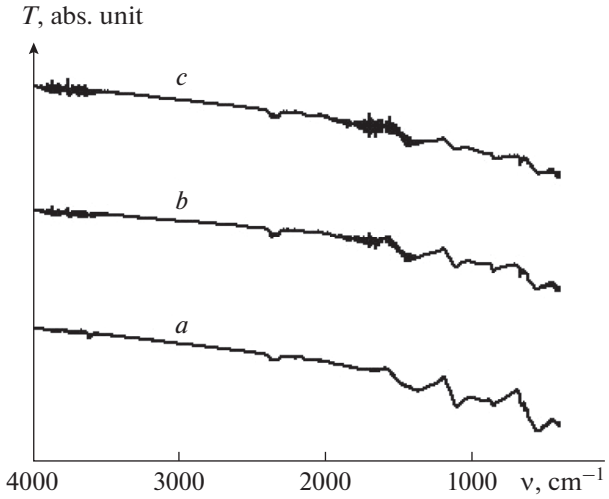

Fig. 2. FT-IR spectrum of (a) $La_{0.9}Sr_{0.1}CoO_3$, (b) $La_{0.6}Sr_{0.4}CoO_3$, (c) $La_{0.5}Sr_{0.5}CoO_3$ prepared at 600°C.

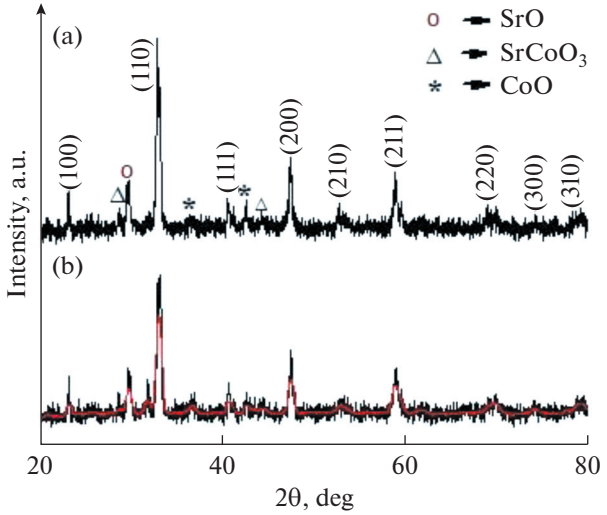

Fig. 3. XRD spectrum of (a) $La_{0.7}Sr_{0.3}CoO_3$ and (b) $La_{0.6}Sr_{0.4}CoO_3$ prepared at 600°C.

structure [31]. Further vibration peak at 1458 cm^{-1} corresponds to lanthanum cobaltate [32]. Another peak at 660 cm^{-1} was found in the oxide phase which indicates spinel phase Co_3O_4 along with the perovskite oxide due to strontium substitution in the perovskite oxide [33]. Some additional peaks were observed in the oxide phase at 855, 1375, and 3595 cm^{-1} due to the vibration of Sr–O [34], the vibration of the carbonate group CO_3^{2-} groups of the O–C–O bond, stretching vibration from O–H bond of the moisture moiety [35] respectively, and another absorption peak at 2350 cm^{-1} is attributed to the stretching vibration of O=C=O [36] but peak at 1100 was un-identified in the IR spectrum of oxides.

XRD Analysis

XRD powder pattern diffraction of synthesized oxides $La_{0.7}Sr_{0.3}CoO_3$ and $La_{0.6}Sr_{0.4}CoO_3$ was carried out in selected phase angle regions of 20 to 80 deg. The multiple XRD reflection peaks matched with their respective strongest peaks through the Joint Committee of Powder Diffraction Standards (JCPDS) file 48-0121. All the XRD spectrum peaks represent the evolution of perovskite-type oxides in both cases. But, along with the perovskite-type oxide peaks some additional peaks (impurity) were observed which are present in trace of quantity such as strontium oxide (SrO) (JCPDS file no. 6-0520), strontium cobalt oxide ($SrCoO_3$) (JCPDS file no. 49-0692) and cobalt oxide (CoO) (JCPDS file 43-1004) in both spectra. Oxides were prepared at 600°C temperature by the sol-gel method using alginic acid as a gelling agent. XRD powder patterns of strontium lanthanum cobaltate oxides are represented in Fig. 3. This figure shows the evolution of the nano-size crystalline oxide structure with the corresponding peaks (100), (110), (111), (200), (210), (211) (220), (300) and (310) XRD planes equal along with the standard JCPDS file No. 48-0121. The perovskite oxides prepared by the sol–gel auto combustion method using alginic acid, calculated values of crystallite size S little more in comparison to Singh et al [37] those oxides prepared by a similar method. The value of crystallite size of Sr-substituted cobaltates is estimated by the full width at half maximum (FWHM) by the most intense peak of the crystal plane using the Debye Scherrer formula $S = \frac{0.9x\lambda}{\beta\cos\theta}$, where β is full width at half maximuma (FWHM), S equal to the crystallite size, and θ equal to the Bragg angle. The value of crystallite size of strontium-substituted cobaltates $La_{0.7}Sr_{0.3}CoO_3$ and $La_{0.6}Sr_{0.4}CoO_3$ is estimated to be ~22, and ~28 nm, respectively.

SEM Analysis

To establish the surface morphology of the oxides, the scanning electron micrographs of $La_{0.6}Sr_{0.4}CoO_3$ at different magnifications were taken and shown in Fig. 4. SEM images showed the agglomerated form of oxide on the surface made up of the fine granules with different nano-scale dimensions (50–100 nm).

Cyclic Voltammetry (CV)

Cyclic voltammograms of fabricated electrodes (oxide/Ni) were recorded at 20 mV/s between potential regions 0 to 0.7 V vs Hg/HgO in 1 M KOH at 25°C and two representative cyclic voltammetric curves of $La_{0.7}Sr_{0.3}CoO_3$ and $La_{0.6}Sr_{0.4}CoO_3$ are shown in Fig. 5. From the CV curves it is clear that there is the formation of redox couple in each case just prior to oxygen evolution reactions. The voltammograms exhibited

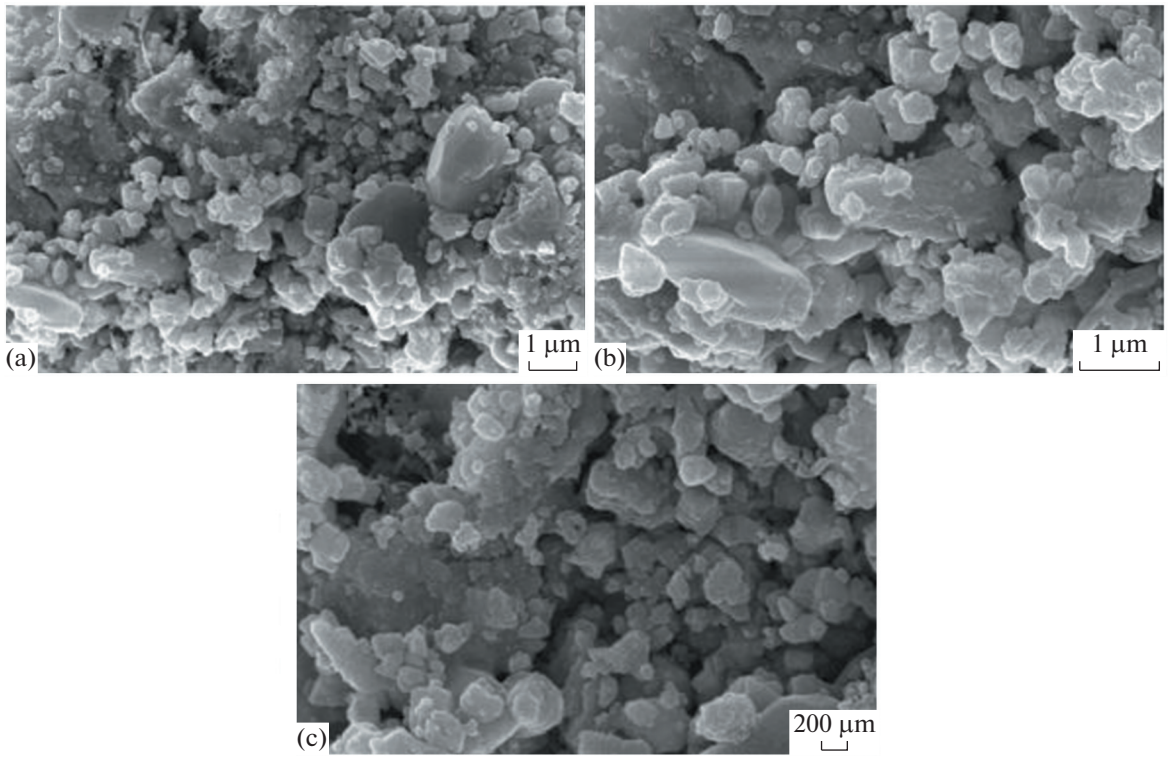

Fig. 4. SEM images of $La_{0.6}Sr_{0.4}CoO_3$ at different magnifications: (a) 20000×, (b) 40000×, and (c) 50000×.

pseudo capacitive with anodic peak potential E_{pa} 399 ± 4 mV, E_{pc} 291 ± 7 mV, ΔE 109 ± 10 mV and These peaks are observed at a fixed potential given in the following Table1.

Oxide Roughness Factors (R_F)

For the determination of the oxide roughness factor (R_F) of each oxide, cyclic voltammograms were recorded at the different scan rates (10, 20, 40, 60, 80, and 100 mV/s) in 1 M KOH solution at 25°C between potentials regions 0.075 and 0.125 V where the contribution of charge transfer reaction is negligible (Fig. 6a). The double layer (C_{dl}) capacitances were measured from the slope of the straight line curve log*j* vs scan rate (Fig. 6b) and the measured value of C_{dl} were 1697, 1347, 1813, 6014, and 2268 μF for the $La_{0.9}Sr_{0.1}CoO_3$, $La_{0.8}Sr_{0.2}CoO_3$, $La_{0.7}Sr_{0.3}CoO_3$, $La_{0.6}Sr_{0.4}CoO_3$, and $La_{0.5}Sr_{0.5}CoO_3$, respectively. The roughness factor for each electrode was calculated from the C_{dl} values by assuming the C_{dl} of smooth oxide surface is 60 μF [38] and given in Table 2. The calculated value of R_F was observed to be almost similar for each oxide electrode. However, 0.4 mol Sr-doped lanthanum cobaltate showed a considerably higher value of R_F (~100) and also showed the most

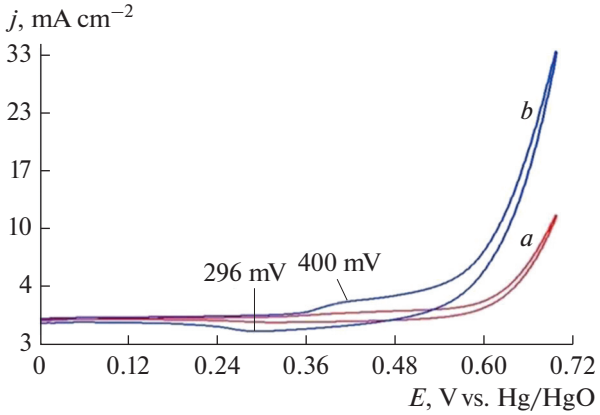

Fig. 5. CV curve of Ni/ (a) $La_{0.7}Sr_{0.3}CoO_3$ and (b) $La_{0.6}Sr_{0.4}CoO_3$ electrode at 20 mV/s in 1 M KOH at 25°C recorded between 0 to 0.7 V.

Table 1. Values of cyclic voltammetric parameters for OER on Sr-substituted lanthanum cobaltate in 1 M KOH at 25°C

Oxides	E_{pa}, mV	E_{pc}, mV	ΔE_p, mV	ΔE_p^0, mV
$La_{0.9}Sr_{0.1}CoO_3$	391	291	100	341
$La_{0.8}Sr_{0.2}CoO_3$	399	297	102	348
$La_{0.7}Sr_{0.3}CoO_3$	400	293	107	347
$La_{0.6}Sr_{0.4}CoO_3$	403	295	108	349
$La_{0.5}Sr_{0.5}CoO_3$	403	277	126	340

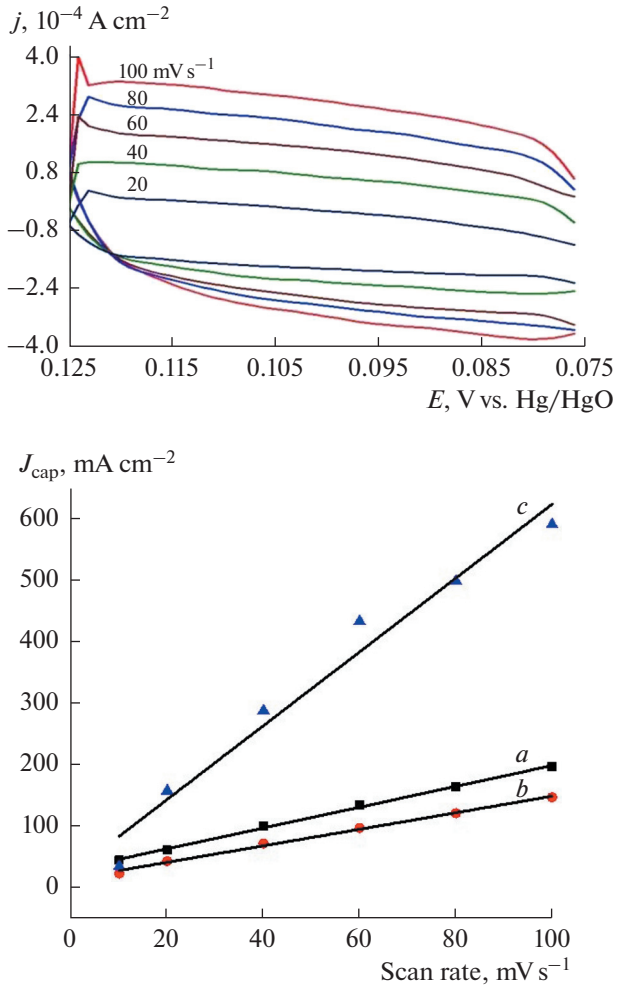

Fig. 6. (a) CV curve of $Ni/La_{0.6}Sr_{0.4}CoO_3$ electrode at different scan rates in 1 M KOH at 25°C recorded between 0.075 to 0.125 V. (b) Plot of charging current density vs. scan rate for (*a*) $Ni/La_{0.9}Sr_{0.1}CoO_3$ (*b*) $Ni/La_{0.8}Sr_{0.2}CoO_3$, and (*c*) $Ni/La_{0.6}Sr_{0.4}CoO_3$ electrodes.

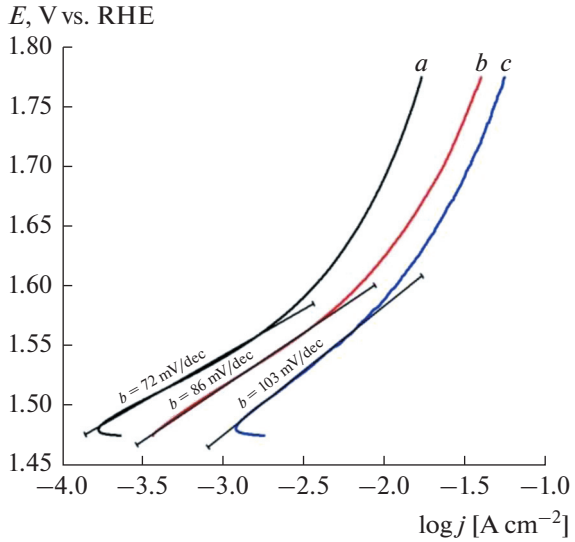

Fig. 7. Tafel polarization curves on Ni/oxide electrodes at 25°C in 1 M KOH: (*a*) $La_{0.8}Sr_{0.2}CoO_3$, (*b*) $La_{0.7}Sr_{0.3}CoO_3$, and (*c*) $La_{0.6}Sr_{0.4}CoO_3$.

active electrode from an O_2 evolution standpoint. The increase in R_F-value with strontium substitution in lanthanum cobaltate matrix prepared by malic acid sol–gel route was also observed by Singh et al. [38].

Electrocatalytic Activity

Electrocatalytic activities for oxygen evolution on Sr-substituted lanthanum cobaltate electrodes were investigated from the Tafel polarization curves in 1 M KOH saturated with Ar-gas at 25°C shown in Fig. 7. The Tafel slope of each oxide electrode was determined from the ratio of potential to the decade of current density values from the polarization curve. The polarization curves showed two Tafel polarization regions, the observed values of the Tafel slopes in lower polarization regions were lies from 72 ± 2 to 126 ± 1 mV dec^{-1}. Sr-substitution in lanthanum cobaltate matrix considerably reduced the Tafel slope value, the maximum reduction in the Tafel slope found in the case of $La_{0.8}Sr_{0.2}CoO_3$ electrode. From the polarization curves of electrodes tested for their OER electrocatalytic activity, it was also apparent that the oxide electrode viz., $La_{0.6}Sr_{0.4}CoO_3$ has the highest value of current density at 0.55 V in an alkaline medium at 25°C. Substitution of Sr in lanthanum cobaltate matrix improved both the apparent current density (j_{app}) as well as the true current density (j_{tr}) appreciably. The maximum improvement was observed in the case of the $La_{0.6}Sr_{0.4}CoO_3$ electrode because of the generation of more concentration of oxygen vacancy in the prepared oxide while reducing the valence of the La site which enhances the number of oxygen vacancies. The prepared oxide electrodes showed a current density very close to those observed by Singh et al. [37, 39]. Higher values of the Tafel slopes most probably due to the lower specific surface area and contribution ohmic resistance [40]. Pavel et al. recently, reported comparatively higher electrocatalytic activity on ruddlesden-popper oxides in 5 M KOH with low values of the Tafel slope (65–70 mV dec^{-1}) and oxygen over potential ~0.27 V at j = 0.1 A cm^{-2} [41], and almost ten times more active towards OER than $La_{1-x}Sr_xCoO_3$ prepared by solid reaction under constant flow of oxygen and studied their electrochemical properties and found formation of dynamically stable active sites during oxygen evolution reaction in alkaline medium and also investigated the effect of Sr-substitution in $LaCoO_3$ matrix for OER and observed that increase of Sr-substitution in $LaCoO_3$ increases current density (J) (1.29, 1.88, 2.58 and 3.88 mA cm^{-2} at E = 1.7 V vs. RHE for x = 0, 0.1, 0.2 and 0.3 mol Sr-sub-

Table 2. Kinetic parameters for O_2 evolution on Ni/oxide electrodes in 1 M KOH (25°C)

Oxide	Tafel slope, mV dec^{-1}	E, mV at j = 10 mA cm^{-2}	j, mA cm^{-2} at E = 850 mV		C_{dl}, μF	R_F
			j_{app}	j_{tr}		
$La_{0.9}Sr_{0.1}CoO_3$	91 ± 3	717	44.83	1.586	1697	28.3
$La_{0.8}Sr_{0.2}CoO_3$	72 ± 2	765	17.04	0.759	1347	22.5
$La_{0.7}Sr_{0.3}CoO_3$	86 ± 2	700	39.82	1.317	1814	30.2
$La_{0.6}Sr_{0.4}CoO_3$	103 ± 3	647	73.07	0.728	6015	100.2
$La_{0.5}Sr_{0.5}CoO_3$	126 ± 1	689	32.72	0.865	2268	37.8

Table 3. Thermodynamic parameters for O_2 evolution on Ni/oxide electrode in 1 M KOH

Electrodes	$\Delta H_{el}^{0\neq}$, kJ mol^{-1} at (η_{O_2} = 0.5 V)	$-\Delta S^{0\neq}$, J deg^{-1}mol^{-1}	α	$\Delta H_c^{0\neq}$, kJ mol^{-1}
$La_{0.9}Sr_{0.1}CoO_3$	26	288	0.64	76.80
$La_{0.6}Sr_{0.4}CoO_3$	24	292	0.57	68.13
$La_{0.5}Sr_{0.5}CoO_3$	12	336	0.46	47.78

stitution respectively) [42]. B.J. Kim et al., studied the functional role of Fe-doping in cobalt based perovskite oxides and reported similar Tafel slopes ~60 mV dec^{-1} and improved activity with Fe-doping due to its synergetic effect [43].

Order of Reaction (p)

For the determination of the order of oxygen evolution reaction, the Tafel polarization curves were recorded at different concentrations of KOH (0.25, 0.5, 0.75, 1.0, and 1.5 M) and the ionic strength of medium (μ = 1.5) was kept constant with the use of KNO_3 as an inert electrolyte at 25°C. The order of reaction was calculated from the slope of log j vs. log[OH$^-$] plot at constant potential (0.8 V). Two representative plots for the $La_{0.6}Sr_{0.4}CoO_3$ and $La_{0.5}Sr_{0.5}CoO_3$ electrodes are given in Fig. 8. The order of reaction for each oxide electrode was found to be approximately unity (~0.7) which indicated that the electrochemical formation of oxygen on electrode/solution interface follow the similar mechanism. A similar kind of mechanism for OER in a KOH medium was also proposed by Singh and co-workers for $La_{1-x}Sr_xCoO_3$ [37, 38] and $La_{1-x}Sr_xMnO_3$ [39] electrodes.

THERMODYNAMIC STUDY

The thermodynamic parameters such as apparent electrochemical activation energy ($\Delta H_c^{0\neq}$) at constant reversible potential, real activation energy ($\Delta H_{el}^{0\neq}$) at constant overpotential (at η_{O_2} 0.5 V) and entropy of reaction ($\Delta S_{el}^{0\neq}$) on fabricated oxide electrodes for OER were determined from the Tafel polarization curves recorded at different temperatures in 1 M KOH solution (Table 3). The value of was estimated from the slope of Arrhenius plot log$j$ vs. $1/T$ shown in Fig. 9. The calculated values of $\Delta H_{el}^{0\neq}$ were 26, 24, and 12 kJ mol^{-1} for $La_{0.9}Sr_{0.1}CoO_3$, $La_{0.6}Sr_{0.4}CoO_3$, and $La_{0.5}Sr_{0.5}CoO_3$ electrodes respectively $\Delta S = 2.303R \times [\Delta H_{el}^{0\neq}/2.303RT + \log j - \log nF\omega C_{OH^-}]$ equation was used for calculation of their entropy of reaction −288, −292, and −336 J deg^{-1} mol^{-1} [39]. This highly

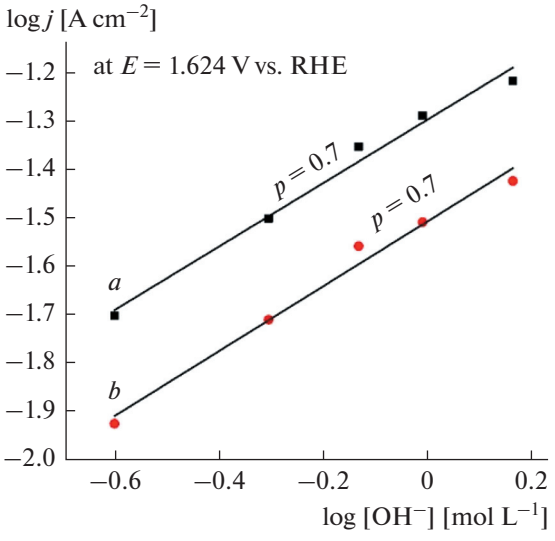

Fig. 8. Plot of log j (at E = 1.624 vs. RHE) vs. log[OH$^-$] at 25°C. (*a*) $La_{0.6}Sr_{0.4}CoO_3$ and (*b*) $La_{0.5}Sr_{0.5}CoO_3$.

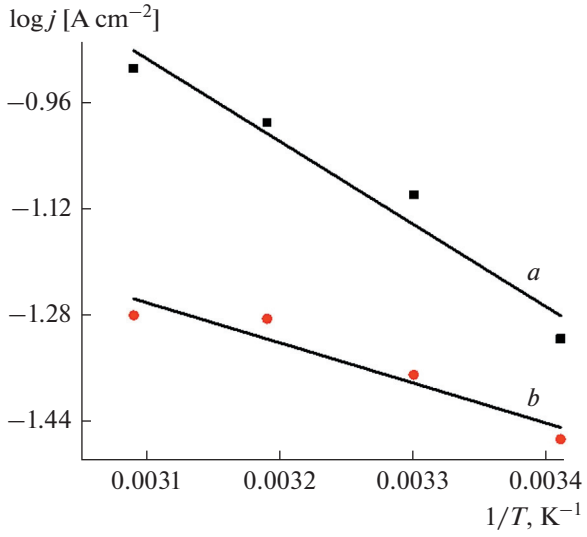

Fig. 9. The Arrhenius plot at 0.8 V in 1 M KOH for (*a*) $La_{0.6}Sr_{0.4}CoO_3$ and (*b*) $La_{0.5}Sr_{0.5}CoO_3$.

negative values entropy of reaction indicates the mechanism of the electrochemical oxygen evolution occurs by the adsorption of the reaction intermediate.

CONCLUSIONS

The present investigation includes the preparation of Sr-substituted lanthanum cobaltate by sol–gel route using alginic acid as a precursor. The formation of the perovskite phase of oxides was established by the TGA, IR, XRD, and SEM analyses. XRD spectra of oxide showed the formation of perovskite as a major phase along with some additional phases in trace amounts. The sol–gel method could be useful for the economical formation of highly active electrocatalysts for oxygen evolution reaction in 1 M KOH solution. Sr-substituted lanthanum cobaltates prepared by the alginic acid sol–gel method are found to considerably have higher electrocatalytic activity than those oxides synthesized by other conventional high-temperature methods. The present investigation also showed that the Sr-substitution in $LaCoO_3$ improves the electrocatalytic activity and recommends them as good candidates for electrocatalytic applications and energy storage devices.

ACKNOWLEDGMENTS

One of the authors B. Lal is grateful to Prof. D.K. Das, Head of the Department of Chemistry, GLA University Mathura for providing the required research facilities.

FUNDING

One of the authors B. Lal is grateful to the UPCST for the financial support through a research grant (CST/CHEM/D-1120 ID-1167).

CONFLICT OF INTEREST

The authors of this work declare that they have no conflicts of interest.

REFERENCES

1. Waser, R., Electrode Kinetics: Reactions, Comprehensive Chemical Kinetics, R.G. Compton (Ed.) Amsterdam, Oxford, New York, Tokyo: Elsevier Sci. Publ. B. V, 1987, vol. 27, *Ber. Bunsengesellschaft Phys. Chem.,* 1989, vol. 93, no. 4, p. 534.
2. Rivas-Murias, B., Fagnard, J.F., Vanderbemden, Ph., Traianidis, M., Henrist, C., Cloots, R., and Vertruyen, B., Spray drying: an alternative synthesis method for polycationic oxide compounds, *J. Phys. Chem. Solid,* 2011, vol. 72, no. 3, p. 158.
3. Maulana, M.I. and Nandiyanto, A.B.D., Economic evaluation of different solvents in the production of $LaCoO_3$ nanoparticles prepared by the co-precipitation method, *Int. J. Adv. Smart Convergence,* 2019, vol. 1, no. 4, p. 7.
4. Alvarez-Galvan, C., Trunschke, A., Falcon, H., Sanchez-Sanchez, M., Campos-Martin, J.M., Schlögl, R., and Fierro, J.L.G., Microwave-assisted co-precipitation synthesis of $LaCoO_3$ nanoparticles and their catalytic activity for syngas production by partial oxidation of methane, *Front. Energy Res.,* 2018, vol. 6, p. 18.
5. Galal, A., Atta, N.F., and Ali, S.M., Investigation of the catalytic activity of $LaBO_3$ (B = Ni, Co, Fe or Mn) prepared by the microwave-assisted method for hydrogen evolution in acidic medium, *Electrochim. Acta,* 2011, vol. 36, no. 16, p. 5722.
6. Mehdizadeh, P., Masjedi-Arani, M., Amiri, O., Al-Nayili, A., and Salavati-Niasari, M., Eco-friendly sonochemistry preparation and electrochemical hydrogen storage of $LaCoO_3/CoO/La_2O_3$ nanocomposite, *Fuel,* 2022, vol. 311, 122544.
7. Samat Rao Somalu, M., Muchtar, A., and Osman, N., Preparation of lanthanum strontium cobalt oxide powder by a modified sol-gel method, *Malaysian J. Anal. Sci.,* 2016, vol. 20, no. 6, p. 158.
8. Popa, M. and Calderon-Moreno, J.M., Lanthanum cobaltite nanoparticles using the polymeric precursor method, *J. Eur. Ceram. Soc.,* 2009, vol. 29, no. 11, p. 2281.
9. Nikam, S.K., Dharmadhikari, D.V., and Athawale, A.A., Comparative study of lanthanum based perovskites synthesized by different methods, in *Springer Proceedings in Physics,* Berlin, Heidelberg: Springer, 2013.
10. Meng, F., Sun, C., Shi, J., Zhang, H., Xu, B., and Ding, Y., Facile synthesis of uniform $LaSrCoO_4$ using amino acid-derived surfactant and its utilization as an excellent cathode material for intermediate tempera-

ture solid oxide fuel cell, *Int. J. Hydrogen Energy,* 2019, vol. 44, no. 2, p. 1122.

11. Qi, X., Lin, Y.S., and Swartz, S.L., Electric transport and oxygen permeation properties of lanthanum cobaltite membranes synthesized by different methods, *Ind. Eng. Chem. Res.,* 2000, vol. 39, no. 3, p. 646.
12. Singh, R.N., Bahadur, L., Pandey, J.P., Singh, S.P., Chartier, P., and Poillerat, G., Preparation and characterization of thin films of $LaNiO_3$ for anode application in alkaline water electrolysis, *J. Appl. Electrochem.,* 1994, vol. 24, p. 149.
13. Vidyasagar, K., Gopalakrishnan, J., and Rao, C.N.R., Synthesis of complex metal oxides using hydroxide, cyanide, and nitrate solid solution precursors, *J. Solid State Chem.,* 1985, vol. 58, no. 1, p. 29.
14. Karimi-Nazarabad, M., Ahmadzadeh, H., and Goharshadi, E.K., Porous perovskite-lanthanum cobaltite as an efficient cocatalyst in photoelectrocatalytic water oxidation by bismuth doped g-C_3N_4, *J. Solar Energy,* 2021, vol. 227, p. 426.
15. Papa, F., Berger, D., Dobrescu, G., State, R., and Ionescu, N.I., Correlation of the Sr-dopant content in $La_{1-x}Sr_xCoO_3$ with catalytic activity for hydrogen peroxide decomposition, *Rev. Roum. Chim.,* 2018, vol. 63, p. 447.
16. Radhakrishnan, M., Padmanathan, N., Esakki Muthu, S., Sivaprakash, P., and Kadiresan, M., Effect of Mn substitution on magnetic behaviour of oxygen defective $LaCoO_3$ perovskite oxide, *Mater. Sci. Eng.,* 2022, vol. 284, 115875.
17. Hussain, S., Javed, M.S., Ullah, N., Shaheen, A., Aslam, N., Ashraf, I., Abbas, Y., Wang, M., Liu, G., and Qiao, G., Unique hierarchical mesoporous $LaCrO_3$ perovskite oxides for highly efficient electrochemical energy storage applications, *Ceram. Int.,* 2019, vol. 45, no. 12, p. 15164.
18. Chumakova, V.T., Marikutsa, A.V., and Rumyantseva, M.N., Nano-crystalline lanthanum cobaltite as a material for gas sensors, *Russ. J. Appl. Chem.,* 2021, vol. 94, no. 12, p. 1651.
19. Suvina, V., Kokulnathan, T., Wang, T.J., and Balakrishna, R.G., Lanthanum cobaltite supported on graphene nanosheets for non-enzymatic electrochemical determination of catechol, *Microchim. Acta.,* 2020, vol. 187, no. 3, p. 1.
20. Lu, Y.C., Li, Y.X., Peng, R., Chen, D.M., Yang, Q.H., and Zhang, S.J., The sintering and electrical properties of $La_{0.5}Sr_{0.5}Co_{0.96}Ni_{0.04}O_{3-\delta}$ ceramics with B_2O_3–CuO addition, *Mater. Sci. Forum,* 2021, vol. 1027, p. 3.
21. Park, J.S. and Kim, Y.B., Synthesis and characterization of nanoporous strontium-doped lanthanum cobaltite thin film using metal-organic chemical solution deposition, *Thin Solid Films,* 2016, vol. 599, p. 174.
22. Zhu, Z., Shi, Y., Aruta, C., and Yang, N., Improving electronic conductivity and oxygen reduction activity in Sr-doped lanthanum cobaltite thin films: cobalt valence state and electronic band structure effects, *ACS Appl. Energy Mater.,* 2018, vol. 1, p. 5308.
23. Hilal, M.E., Şanlı, S.B., Dekyvere, S., Çakmak, G., Younus, H.A., Pişkin, F., Verpoort, F., and Pişkin, B., A dual-doping strategy of $LaCoO_3$ for optimized oxygen evolution reaction toward zinc-air batteries application, *Int. J. Energy Res.,* 2022, vol. 46, no. 15, p. 22014.
24. Yu, H.C., Fung, K.Z., Guo, T.C., and Chang, W.L., Syntheses of perovskite oxides nanoparticles $La_{1-x}Sr_xMO_{3-\delta}$ (M = Co and Cu) as anode electrocatalyst for direct methanol fuel cell, *Electrochim. Acta,* 2004, vol. 50, nos. 2–4, p. 811.
25. Kalubarme, R.S., Park, G.E., Jung, K.N., Shin, K.H., Ryu, W.H., and Park, C.J., $LaNi_xCoO_{3-\delta}$ perovskites as catalyst material for non-aqueous lithium-oxygen batteries, *J. Electrochem. Soc.,* 2014, vol. 161, no. 6, p. 880.
26. Sun, C., Alonso, J.A., and Bian, J., Recent advances in perovskite-type oxides for energy conversion and storage applications, *Adv. Energy Mater.,* 2020, vol. 11, no. 2, 2000459.
27. Sun, X., Meng, Z., Hao, Z., Du, Z., Xu, J., Nan, H., Shi, W., Zeng, F., Hu, X., and Tian, H., Efficient fabrication of flower-like core-shell nanochip arrays of lanthanum manganate and nickel cobaltate for high-performance supercapacitors, *J. Colloid Interface Sci.,* 2023, vol. 630, p. 618.
28. Okugawa, T., Ohno, K., Noda, Y., and Nakamura, S., Weakly spin-dependent band structures of antiferromagnetic perovskite $LaMO_3$ (M = Cr, Mn, Fe), *J. Phys. Condens. Matter,* 2018, vol. 30, no. 7, p. 75502.
29. Enache, S., Dragan, M., Varlam, M., and Petrov, K., Electronic percolation threshold of self-standing Ag-$LaCoO_3$ porous electrodes for practical applications, *Materials,* 2019, vol. 12, no. 15, p. 2359.
30. Zhang, X., Li, F., and Zheng, R., Growth and optimization of hybrid perovskite single crystals for optoelectronics/electronics and sensing, *J. Mater. Chem. C,* 2020, vol. 8, no. 40, p. 13918.
31. Sun, M., Jiang, Y., Li, F., Xia, M., Xue, B., and Liu, D., Dye degradation activity and stability of perovskite-type $LaCoO_{3-x}$ (x = 0–0.075), *Mater. Trans.,* 2010, vol. 51, no. 12, p. 2208.
32. Sarker, A.R., Synthesis of high qulity $LaCoO_3$ crystals using water-based sol–gel method, *Int. J. Mat. Sci. Appl.,* 2015, vol. 4, no. 3, p. 159.
33. Zhou, C., Feng, Z., Zhang, Y., Hu, L., Chen, R., Shan, B., Yin, H., Wang, W.G., and Huang, A., Enhanced catalytic activity for NO oxidation over Ba doped $LaCoO_3$ catalyst, *RSC Adv.,* 2015, vol. 5, no. 36, p. 28054.
34. Alhokbany, N., Almotairi, S., Ahmed, J., Al-Saeedi, S.I., Ahamad, T., and Alshehri, S.M., Investigation of structural and electrical properties of synthesized Sr-doped lanthanum cobaltite ($La_{1-x}Sr_xCoO_3$) perovskite oxide, *J. King Saud Univ. Sci.,* 2021, vol. 33, no. 4, 101419.
35. Pecchi, G., Campos, C., Jiliberto, M.G., Moreno, Y., and Pena, O., Doping of lanthanum cobaltite by Mn thermal, magnetic, and catalytic effect, *J. Mater. Sci.,* 2008, vol. 43, no. 15, p. 5282.
36. Irshad, M., Idrees, R., Siraj, K., Shakir, I., Rafique, M., and Ain, Q., and Raza, R., Electrochemical evaluation of mixed ionic electronic perovskite cathode $LaNi_{1-x}Co_xO_{3-\delta}$ for IT-SOFC synthesized by high-

temperature decomposition, *Int. J. Hydrogen Energy,* 2021, vol. 46, no. 17, p. 10448.

37. Singh, R.N. and Lal, B., Electrocatalytic characterization of new $La_{1-x}Sr_xCoO_3$ films on Pt for use as oxygen anode in alkaline solutions, *Ind. J. Chem. A,* 2010, vol. 40, no, 10, p. 1037.
38. Singh, N.K., Tiwari, S.K., and Singh, R.N., Electrocatalytic properties of lanthanum manganites obtained by a novel malic acid-aided route, *Int. J. Hydrogen Energy,* 1998, vol. 23, no. 9, p. 775.
39. Lal, B., Raghunandan, M.K., Gupta, M., and Singh, R.N., Electrocatalytic properties of perovskite-type obtained by a novel stearic acid sol-gel method for electrocatalysis of evolution in KOH solutions, *Int. J. Hydrogen Energy,* 2005, vol. 30, no. 7, p. 723.
40. Porokhin, S.V., Nikitina, V.A., Aksyonov, D.A., Filimonov, D.S., Pazhetnov, E.M., Mikheev, I.V., and Abakumov, A.M., Mixed cattion perovskite $La_{0.6}Ca_{0.4}Fe_{0.7}Ni_{0.3}O_{2.9}$ as stable and efficient catalyst for oxygen evolution reaction, *ACS, Catal.,* 2021, vol. 11, p. 8338.
41. Sinitsyn, A.P., Kuznetsov, V.V., Filatova, A.E., and Levchenko, V.S., Ruddlesden–Popper oxides $LaSrM^1_{1-x}M^2_xO_{4\pm\delta}$ (M^1, M^2—Fe, Co, Ni) synthesized by the spray pyrolysis method as promising electrocatalysis for oxygen evolution reaction, *Energies,* 2022, vol. 15, p. 8315.
42. Lopes, P.P., Chung, D.Y., Rui, X., Zheng, H., He, Haiying., Martins, P.F.B.D., Strmcnik, D., Stamenkovic, V.R., Zapol, P., Mitchell, J.F., Klie, R.F., and Markovic, N.M., Dynamically active sites from surface evolution of perovskite materials during the oxygen evolution reaction, *J. Am. Chem. Soc.,* 2021, vol. 143, p. 2741.
43. Kim, B.J., Fabbri, E., Abott, D.F., Cheng, X., Clark, A.H., Nachtegaal, M., Borlof, M., Castelli, I.E., Graule, T., and Schmidt, T.J., Functional role of Fe-doping in Co-based perovskite oxide catalysts for oxygen evolution reaction, *J. Am. Chem. Soc.,* 2019, vol. 141, p. 5231.